Differences between the Lateral Organization of Conventional and Inositol Phospholipid-anchored Membrane Proteins. A Further Definition of Micrometer Scale Membrane Domains

Michael Edidin* and Iwona Stroynowski‡

*Department of Biology, The Johns Hopkins University, Baltimore, Maryland 21218; and ‡Biology Division, California Institute of Technology, Pasadena, California 91125

Abstract. Plasma membranes of many cells appear to be divided into domains, areas whose composition and function differ from the average for an entire membrane. We have previously used fluorescence photobleaching and recovery to demonstrate one type of membrane domain, with dimensions of micrometers (Yechiel, E., and M. Edidin. 1987. *J. Cell Biol.* 105: 755–760). The presence of membrane domains is inferred from the dependence of the apparent mobile fraction of labeled molecules on the size of the membrane area probed. We now find that by this definition classical class I MHC molecules, H-2D^b, are concentrated in domains in the membranes of K78-2 hepatoma cells, while the nonclassical class I-related molecules, Qa-2, are free to pass the boundaries of these domains. The two proteins are highly homologous but differ in their mode of anchorage to the membrane lipid bilayer. H-2D^b is anchored by a transmembrane peptide, while Qa-2 is anchored by a glycosylphosphatidylinositol (GPI) anchor. A mutant class I protein with its external portion derived from Qa-2 but with transmembrane and cytoplasmic sequences from a classical class I molecule shows a dependence of its mobile fraction on the area of membrane probed, while a mutant whose external portions are a mixture of classical and nonclassical class I sequences, GPI-linked to the bilayer, does not show this dependence and hence by our definition is not restricted to membrane domains.

CELL surface membranes are differentiated into patches or domains whose composition, physical properties, and function differ from the average for an entire cell surface. Some membrane domains, for example the basal/lateral or apical surfaces of morphologically polarized epithelial cells (Rodriguez-Boulan and Nelson, 1989), are easily seen by light microscopy and even domains as small as 50–100-nm clusters of glycolipids are seen in electron micrographs of erythrocyte membranes (Thompson and Tillack, 1985). Other membrane domains of various sizes are also detected in cell surface membranes (reviewed in Edidin, 1990*a*) though they usually cannot be imaged in micrographs. Instead, their presence is inferred from the behavior of membrane probes that is not predicted by, or consistent with, the properties of a continuous, fluid, lipid bilayer. Such domains then are defined by the experiments that detect them, for example in terms of heterogeneities of fluorescence lifetimes (Klausner et al., 1980; Karnovsky et al., 1982) or of lateral diffusion coefficients (Wolf et al., 1981; Handyside et al., 1982; Wolf et al., 1988).

We have defined one type of domain using fluorescence photobleaching and recovery (FPR)[1] to measure the mobile fractions of a lipid probe and of labeled proteins in human fibroblast cell surface membranes (Yechiel and Edidin, 1987). In an FPR experiment, diffusion of a fluorescent label is measured in terms of the return of fluorescence to a small area of the surface that has been partly bleached by a focused laser beam. The time for recovery of fluorescence is expected to depend upon the area bleached, but the extent of recovery of fluorescence, which depends on the fraction of mobile molecules in the labeled population, is expected to be independent of the area. While this is true in synthetic bilayer membranes, we found that in human fibroblast plasma membranes the mobile fraction of a fluorescent lipid analogue, NBD-PC and of antibody-labeled proteins does depend on the area bleached, even though these areas, 1–25 μm^2 are significantly smaller than that of the cell surface, 2–300 μm^2 (Yechiel and Edidin, 1987). These observations together with a detailed analysis of diffusion coefficients were interpreted in terms of protein-rich domains, ~2 μm in diameter, interspersed with lipid-rich regions of membrane. Structures of about this size were in fact observed when large areas (100–200 μm^2) of membrane brightly labeled with NBD-PC were repeatedly bleached and then observed with low-intensity laser light.

A better definition of the structure of the micrometer scale domains defined by FPR experiments could be gained by the study of a single protein with variant forms of anchoring to

1. *Abbreviations used in this paper*: FRP, fluorescence photobleaching and recovery; GPI, glycosylphosphatidylinositol; MHC, major histocompatibility complex.

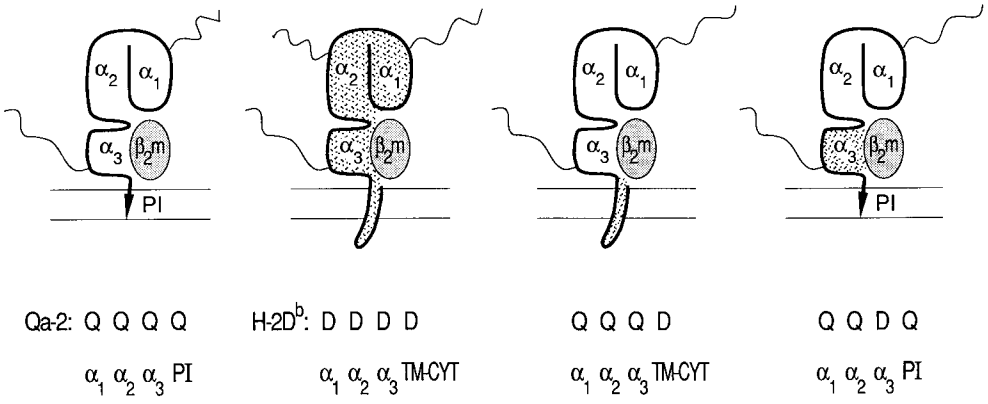

Figure 1. The predicted organization of the Qa-2, H-2D^b, and chimeric molecules QQQD and QQDQ. The N-linked carbohydrates (marked by *wavy lines*) are attached to residues 86 (in Qa-2 and H-2D^b), 176 (in H-2D^b), and 256 (in Qa-2 and H-2D^b). All are predicted to be accessible to solvent in the crystallographic HLA-A2 model (Bjorkman et al., 1987). The 24 residues of hydrophobic transmembrane domain of H-2D^b are followed by 42 amino acids of highly charged cytoplasmic tail. The GPI of Qa-2 is thought to be attached to the COOH-terminal residue of the alpha 3 domain or to a downstream amino acid encoded by exon 5 (Ulker et al., 1990). Qa-2 is expressed on K78-2 transfected HEPA OVA cells. QQQD is expressed on K123-12 cells and QQDQ is expressed on K123-13 cells. All of these cells express H-2D^b.

the membrane bilayer. Class I major histocompatibility complex (MHC) molecules allow such a comparison since there are many variants and mutants of each of the molecule's domains, extracellular, transmembrane, and cytoplasmic. Here we compare the diffusibility of two class I MHC molecules which are highly homologous in their external domains: a classical class I molecule, H-2D^b, that is anchored to the lipid bilayer by a transmembrane peptide, and a nonclassical class I-related molecule, Qa-2 (Stroynowski, 1990), that is glycosylphosphatidylinositol (GPI)-anchored to the bilayer (Stroynowski et al., 1987). These molecules show different behavior in FPR experiments when expressed in the same cell surface. The mobile fraction of H-2D^b antigens depends upon the area of the membrane interrogated in an FPR experiment, while the mobile fraction of Qa-2 antigens is independent of this area. Using our operational definition of a membrane domain we conclude that Qa-2 antigens are able to cross domain boundaries in the time (minutes) of an FPR experiment. This suggests that transmembrane and cytoplasmic regions of proteins are important in keeping them organized in micrometer scale domains.

Materials and Methods

Cells and Genes

The recipient HEPA-OVA mouse hepatoma cells (Darlington et al., 1980) express endogenous *H-2D^b* MHC molecules, but not H-2K^b molecules (Fig. 1).

K78-2 are HEPA OVA cells transfected with a Qa-2 gene (Q7^b). They express transmembrane-spanning H-2D^b and glycophospholipid-linked Qa-2 molecules (Fig. 1).

K123-12 are HEPA-OVA transfected with and expressing the product of a hybrid class I gene specifying the alpha 1, alpha 2, and alpha 3 domains of Qa-2 and transmembrane and cytoplasmic domains identical to H-2D^b (Fig. 1). A subpopulation of cells was selected by three rounds of flow cytometric sorting for the brightest 5–10% of labeled cells (Epics 752 flow cytometer; Epics Division, Coulter Corp., Hialeah, FL). The original population consisted of cells only about two times brighter than unlabeled cells. The population of selected cells was a mixture of dim (40%) cells and cells about eight times brighter than the original (60%). This mixture was not resolved by sorting and separately culturing bright and dim cells. Hence, K123-12-3 was used for all FPR experiments.

K123-13 are HEPA-OVA transfected with and expressing the product of a hybrid class I gene specifying the alpha 1 and alpha 2 domains of Qa-2, and an alpha 3 domain identical to H-2D^b but GPI-linked to the bilayer (Fig. 1). Bright cells were selected in a manner similar to the selection for K123-12. The best populations consisted of a majority of cells about four times brighter than the unlabeled controls. Sorting of the brightest and dimmest cells show that the bright cells in this population give rise to populations of bright cells. K123-13-4 were used for FPR experiments.

The chimeric genes transfected into K123-12 and K123-13 were constructed by D. Mann and I. Stroynowski (unpublished data). The genes were constructed by exon shuffling of a Qa-2 gene (Q7^b) and the H-2L^d gene using Hind III restriction enzyme sites (introduced into the intron between exon 4 and exon 5 in Q7^b and H-2L^d) and Bam HI sites (in the intron between exon 4 and exon 5, and downstream from exon 8). Because the amino acid sequence of H-2L^d is identical to that of H-2D^b in alpha 3, transmembrane and cytoplasmic regions, and because our endogenous classical class I molecule is H-2D^b and not H-2L^d, we will refer to the relevant portions of the hybrid proteins as if they were derived from H-2D^b and not from H-2L^d (Fig. 1). Transfections were performed as previously described (Stroynowski et al., 1987).

All cells were cultured in Dulbecco's modified Eagle's medium (Gibco Laboratories Inc., Grand Island, NY) 10% in fetal calf serum (Reiheis, Armour, Chicago, IL) containing 300 μg/ml G418 (Gibco Laboratories Inc.).

Antibodies and Antibody Fragments

Fab fragments of mAb 20-8-4 (Ozato and Sachs, 1980) were used to label Qa-2 and hybrid antigens. Fab fragments of mAb 28-14-8 were used to label the H-2D^b antigens. The Fab fragments were prepared by brief (10 min) digestion with papain (Sigma Chemical Co., St. Louis, MO) at pH 5.5 and 37°C, followed by chromatography on Sephadex G-100 to remove peptide fragments and the bulk of the undigested IgG. The Fab peak was passed over protein A–Sepharose to remove any traces of IgG. Fab fragments at 5 mg/ml were labeled by reaction with 15 μg fluorescein isothiocyanate (Molecular Probes Inc., Eugene, OR)/mg protein in Na_2CO_3 buffer, pH 9.5, for 30 min in ice. Unreacted fluorescein was removed by passing the conjugates over Sephadex G-25.

Labeling of cells by the conjugates was reduced to <20% of maximum by excess unlabeled IgG as determined by flow cytometry.

Conjugates were ultracentrifuged for 1 h at 100,000 *g* (Airfuge, Beckman Instruments, Inc., Fullerton, CA) before use in FPR experiments (Bierer et al., 1987).

Fluorescent Lipid Analogues

NBD-PC (1-palmitoyl-2-[6-[7-nitro-2-1-3-benzoxadiazol-4-y l)amino]caproyl] phosphatidylcholine) was obtained from Avanti Biochemical, Inc. (Birmingham, AL). It was diluted into medium from an ethanol stock solution to give a final concentration of 0.1 μg/ml dye and 1% ethanol. Cells were labeled in this solution for 30 min on ice. diI C16 (1,1'-dihexadecyl-3,3,3,3'-tetramethylindocarbocyanine perchlorate) was obtained from Molecular Probes, Inc. It was diluted into medium from a 100 μg/ml stock in ethanol to give a final concentration of 0.5–1.0 μg/ml diI.

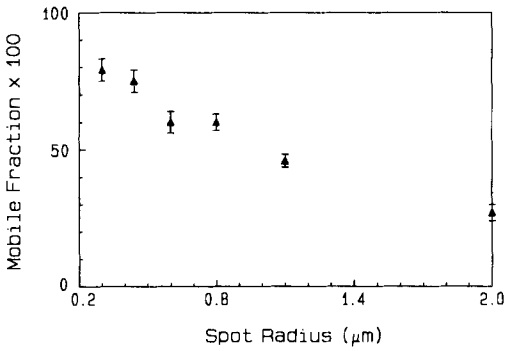

Figure 2. The mobile fractions of NBD-PC in K78 hepatoma cell membranes when measured with laser spots of different radii. Data, shown as mean ±SEM, are pooled from three experiments. One experiment consists of one day's measurements that may be made on one or more cell samples.

FPR

Our spot FPR machine and software have been described elsewhere (Wolf and Edidin, 1981). The machine is based on a Leitz Ortholux microscope, coupled to a 3.5 W argon ion laser (Coherent Radiation Inc., Palo Alto, CA). An E G & G photon counter outputs pulses to a custom counter/timer board controlled by software. The measuring laser power density was typically 0.4–4 kW/cm^2; the bleaching power density was 0.8–1 MW/cm^2.

Cells to be used for FPR were grown on 25-mm square coverslips in medium containing 10–30% of the supernatant from Con A-stimulated rat T cells. Exposure to this crude interferon-containing medium increased expression of Qa-2 and H-2D^b about two-fold after 24 h.

Regions for measurement were selected in bright field (phase contrast) and were chosen to be away from the nucleus. No selection was made in terms of fluorescence intensity which varied three- to fourfold in the cultures used. Only one measurement was made for each cell. Occasionally the region chosen was very bright, five to ten times greater than average. Fluorescence in these spots was always immobile and presumably was due to fluorescent debris stuck to the cells.

Determination of the Radii of the Spots Produced by Different Objectives

The accurate determination of laser spot size is critical to the interpretation of our experiments. We determined the spot sizes produced by different objectives by a variant of method three of Schneider and Webb (1981), scanning the intensity profile of an expanded image of the laser spot, but using a video camera instead of film. The expanded image was obtained by substituting a piece of plain glass for the dichroic mirror and filter so that the laser light could be reflected off of a first surface mirror and projected into the video camera. Scratches in the mirror allowed careful focusing onto its surface. The scans were recorded using a video line analyzer (model 321; Colorado Video, Boulder CO) whose output was recorded on a chart recorder. The tracings of intensity profiles were calibrated against scans of a stage micrometer divided into 2-μm rulings. The system's response, calibrated with neutral density filters, is linear down to 4% of the maximum (subsaturating) intensity used. Hence we can directly measure the e^{-2} height above baseline and determine the beam diameter at this level. We have also used the approach of Schneider and Webb (1981), measuring the height of the peak with a 50% transmission neutral density filter in the light path and using this height to define the diameter of the unfiltered image. Results by the two methods agreed within 20% or less despite small inaccuracies in orienting the filters normal to the laser beam.

If we have accurately measured spot sizes, and there is no systematic error in measurement, then, while $t_{1/2}$ ought to vary with objective, all objectives should give the same calculated D for diffusion of a protein in a homogeneous model system. We made a simple model by making a solution of 2% fluorescent IgG in water/98% anhydrous glycerol (wt/wt). The mixture was equilibrated for 4 d before use in FPR. Its viscosity at 23°C was 654 ± 40 centipose. Values of D (averaged from 10 measurements) for different objectives were: 90× (0.35>μm-spot radius) 5 × 10^{-10} cm^2 · s^{-1}; 63× (0.45-μm-spot radius) 4 × 10^{-10} cm^2 · s^{-1}; 40× (0.75-μm-spot radius) 4 × 10^{-10} cm^2; 22× (1.3-μm-spot radius) 5 × 10^{-10} cm^2. These D differ <20% from D calculated from the published D for IgG in water (4 × 10^{-7} cm^2 · s^{-1}) and the viscosity of our glycerol solution corrected for the measurement temperature, 20°C. Complete recovery of fluorescence was seen for all spot sizes (average mobile fraction = 1).

We found no dependence of the measured diffusion coefficient on the depth of bleaching in the range 25–75% for any objective except the 90×. The 90× objective gives higher D with increasing bleach depths. This probably reflects the fact that our program for analysis of FPR curves extrapolates the observed recovery back to a time in the mid-point of the bleach. We have found, using 95% glycerol solutions that the 90× objective can reliably resolve D of 1–2 × 10^{-9} cm^2 · 2^{-1}, but that larger D are not reliably determined with this objective. Instead, the recovery curves are truncated so that D appears to be ~10-fold smaller than it actually is.

Results

The experiment that we originally used to define domains in fibroblast plasma membranes (Yechiel and Edidin, 1987) shows that the similar domains exist in the plasma membranes of K78-2 hepatoma cells. Data from three experiments on the relationship between mobile fraction and beam radius for NBD-PC-labeled K78-2 cells and covering a range of beam radii from 0.3 to 1.7 μm are summarized in Fig. 2. While there is a range of mobile fractions among cells examined at any one beam radius, it is clear that the apparent mobile fraction decreases as the size of the illuminated region of the cell surface is increased. This is not an artifact of the microscope optics since it is not seen for NBD-PC incorporated into large, cell-sized, liposomes (Yechiel and Edidin, 1987), for diffusion of fluorescence protein in glycerol

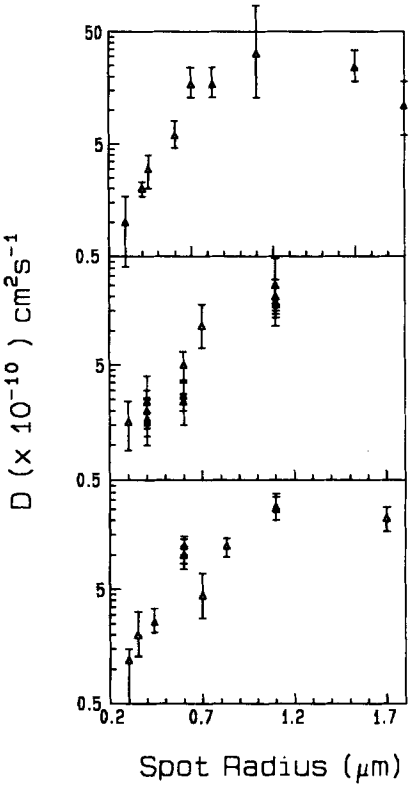

Figure 3. Diffusion coefficients, D, in K78 hepatoma cell membranes as a function of laser spot size of: NBD-PC (*top*); H-2D^b (*center*); and Qa-2 (*bottom*). Values are geometric means ± 95% confidence intervals.

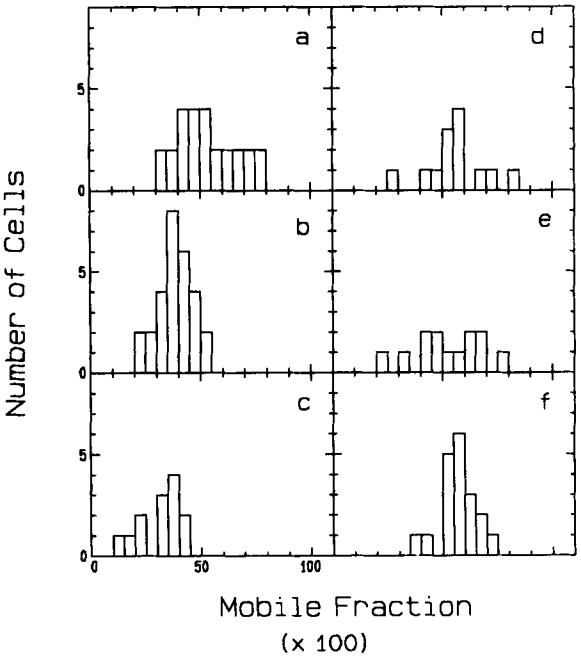

Figure 4. The mobile fractions of H-2D^b (*a–c*) or Qa-2 (*d–f*) molecules in membranes of individual K78 hepatoma cells when measured with laser spots of different radii. (*a*) H-2D^b. Spot radius, 0.4 μm (63× objective). Average mobile fraction is 0.53 ± 0.13. (*b*) H-2D^b. Spot radius, 0.6 μm (40× objective). Average mobile fraction is 0.39 ± 0.08. (*c*) H-2D^b. Spot radius, 1.1 μm (22× objective). Average mobile fraction is 0.32 ± 0.12. (*d*) Qa-2. Spot radius, 0.3 μm (90× objective). Average mobile fraction is 0.56 ± 0.14. (*e*) Qa-2. Spot radius, 0.7 μm (40× objective). Average mobile fraction is 0.53 ± 0.15. (*f*) Qa-2. Spot radius, 1.1 μm (22× objective). Average mobile fraction is 0.54 ± 0.15.

(Materials and Methods) or when comparing the behavior of another lipid analogue, dil C16, in K78-2 cells (see below).

The diffusion coefficients, *D*, of the lipid analogue also changed with spot size, increasing from ~1.0 × 10^{-10} cm^2/s^{-1} for a spot of 0.3 μm radius to ~25 × 10^{-10} cm^2 · s^{-1} for a spot of 1.8 μm radius. (Fig. 3, *top*). Though the data sets were smaller than those used previously (Yechiel and Edidin, 1987), we could show that when measuring spots of small radii (0.4 and 0.7 μm) *D* increased with increasing concentration of the lipid probe, measured as fluorescence intensity before bleaching (data not shown).

Unlike NBD-PC, the fluorescent phospholipid analogue dil C16 has a fluorescent headgroup and unmodified hydrophobic (alkyl) chains. The diffusion coefficient of this analogue is sensitive to the state of membrane lipids (Klausner and Wolf, 1981) but in fibroblast membranes its mobile fraction does not vary with changing spot size (Yechiel and Edidin, 1987). The mobile fraction of dil C16 in hepatoma cell membranes varied only slightly when measured with different size laser spots. 36 measurements using an 0.6-μm spot radius gave R = 0.66 ± 0.18; 31 measurements of dil C 16 using a 1.1-μm-spot radius gave R = 0.60 ± 0.16. These values do not differ significantly from one another. *D* for the two sets of measurements differed by ~50% (6 × 10^{-10} cm^2 · s^{-1} for the 0.6-μm spot and 10 × 10^{-10} cm^2 for the 1.1-μm spot). In a second experiment with only 5–10 cells measured for each spot size R of dil C16 was 0.64 ± 12, when measured in a spot of 0.45-μm-radius spot, 0.72 ± 11 when measured in a spot of 0.75 μm radius and 0.69 ± 8 when measured in a spot of 1.3 μm radius.

Having used a fluorescent phospholipid analogue to experimentally define domains in K78-2 cell membranes, we next looked to see if the classical class I MHC molecules of these cells, the H-2D^b molecules, were also organized into domains. Since in an FPR experiment the estimated mobile fraction is affected by the ratio of specific label to cell autofluorescence, we grew cells in medium containing interferon for 24–48 h before using them for FPR. Flow cytometric measurements showed that this treatment increased the level of surface H-2D^b approximately twofold (data not shown). Fig. 4, *a–c*, compares the range of mobile fractions of H-2D^b molecules in populations of cells where lateral diffusion was measured in spots of 0.4, 0.6, and 1.1 μm radius. Again, a marked shift to lower mobile fractions is seen when larger spot sizes are used. Data from four sets of measurements on different days are summarized in Fig. 5. In each experiment there is a trend to lower mobile fractions with increasing size of the surface area in which fluorescence in measured and bleached. The diffusion coefficient of the labeled H-2D^b molecules increased ~20-fold over the range of spot sizes used in these experiments (Fig. 3, *center*).

We had previously observed that *D* of membrane proteins was inversely related to the protein concentration in the area bleached by a small diameter laser beam (Yechiel and Edidin, 1987). This was also the case for H-2D^b. *D* measured with a small, 0.6 μm radius, laser beam was lower with increasing fluorescence intensity (taken as indicating the concentration of molecules in the region probed) but there was no obvious relationship of *D* with intensity for measurements with a 1.1-μm-radius spot (data not shown).

K78-2 cells are transfected with the Q7 gene and express the GPI-linked class I–related molecule, Qa-2. These cells were better labeled for Qa-2 than for H-2D^b. Hence, we were able to measure mobile fractions of labeled Qa-2 molecules in cells that had not been treated with crude interferon as well as in cells that had been treated to raise surface expression of Qa-2. Distributions of mobile fractions of Qa-2 for 1-d measurements are shown in Fig. 4, *d–f*, for spot radii of 0.30, 0.7, and 1.1 μm. These distributions and their means do not change with increasing spot size remaining ~0.5, over a range of spot radii from 0.3 to 1.8 μm (Fig. 6). In contrast, *D* of Qa-2 antigens depended upon spot size in the same way as *D* of NBD-PC and of H-2D^b molecules (Fig. 3, *bottom*).

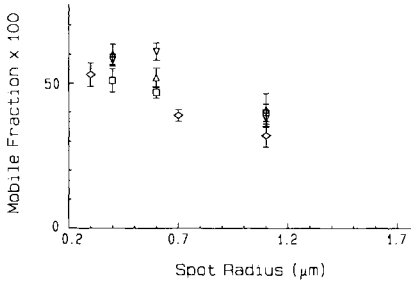

Figure 5. The mobile fractions of Fl-Fab-labeled H-2D^b molecules in K78 hepatoma cell membranes when measured with laser spots of different radii. Data from four experiments are shown as mean ± SEM. Values from one experiment all have the same symbol.

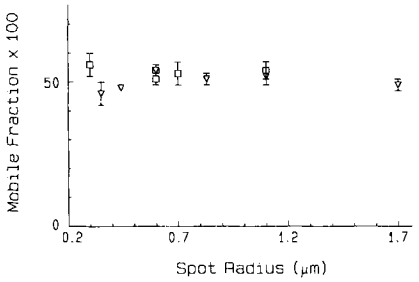

Figure 6. The mobile fractions of Fl-Fab-labeled Qa2 molecules in K78 hepatoma cell membranes when measured with laser spots of different radii. Data from two experiments are shown as mean ± SEM. Values from one experiment all have the same symbol.

However, D was independent of Qa-2 concentration, measured as fluorescence intensity, even when small regions were probed, using a 0.4- or 0.6-μm spots (data not shown).

The results on Qa-2 antigens suggest that the transmembrane domain and/or the cytoplasmic tail of H-2D^b keeps it confined to domains. To test this we measured the lateral diffusion of two hybrid molecules expressed on the surface of HEPA-OVA cells after transfection with the appropriately modified class I MHC genes. Fig. 1 diagrams the predicted domain organization of the two hybrids. The hybrid expressed in K123/12 consists of the exodomains of the Qa-2 molecule joined to the transmembrane and cytoplasmic domains with the sequence of the conventional H-2 molecule, H-2D^b. The hybrid expressed in K123/13 consists of the first two external domains, alpha-1 and alpha-2 of the Qa-2 molecule, the third external domain, alpha 3, with the sequence of H-2D^b and the GPI membrane linkage specified by a portion of the Q7 gene. Fig. 7, *a* and *b* compares the distributions of mobile fractions of the construct molecule, K123/12, peptide linked to the bilayer, measured with 0.6- and 1.1-μm-radius spots. The mobile fraction of this molecule is significantly larger when measured with the 0.6-μm spot than when measured with the 1.1-μm spot ($R = 0.50 \pm 0.08$ vs. $R = 0.37 \pm 0.11$). On the other hand, the mobile fraction of the GPI-linked construct, K123/13, is no different when measured with the 0.6-μm spot than when measured using the 1.1-μm spot ($R = 0.42 \pm 0.16$ vs. $R = 0.46 \pm 14$, respectively) (Fig. 7, *c* and *d*). D of both constructs was $\sim 5 \times 10^{-10}$ cm$^2 \cdot$ s^{-1} when measured with the 0.6-μm spot and $\sim 2 \times 10^{-9}$ cm$^2 \cdot$ s^{-1} when measured with the 1.1-μm spot.

Discussion

We have previously shown that the cell surface of fibroblast membranes contains membrane domains experimentally defined by the dependence of the mobile fraction, R, and the diffusion coefficient, D, of a fluorescent lipid analogue, NBD-PC on the size of the laser spot used for FPR measurements of lateral diffusion. The mobile fraction decreased with increasing spot size, while D increased with increasing spot size. These results, together with fluorescence images of labeled cell surfaces, led to a model of membrane domains rich in membrane proteins, separated by regions relatively poor in proteins. FPR measurements of membrane proteins labeled with fluorescent Fab fragments also showed a dependence of both R and D on spot size.

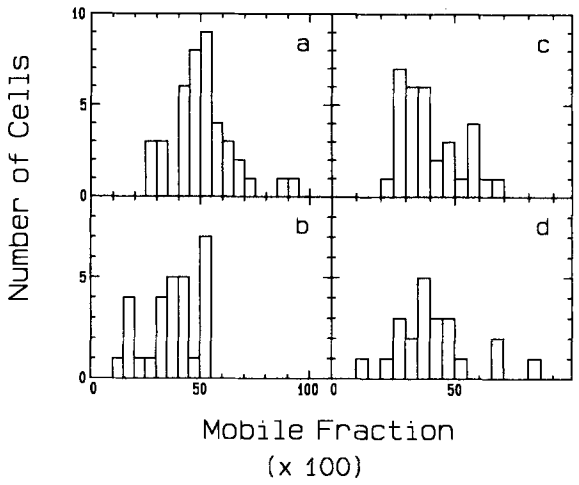

Figure 7. The mobile fractions, measured with laser spots of different radii, of the transmembrane peptide-anchored Qa-2 molecule expressed in K123-12-4 hepatoma cells (*a* and *b*). (*a*) Spot radius, 0.6 μm (40× objective). Average mobile fraction is 0.50 ± 0.08. $D = 4 \times 10^{-10}$ cm$^2 \cdot$s^{-1}. (*b*) Spot radius, 1.1 μm (22× objective). Average mobile fraction is 0.37 ± 0.11. $D = 25 \times 10^{-10}$ cm$^2 \cdot$s^{-1}. The GPI-anchored Qa-2/H-2D hybrid molecule expressed in K123-13-4 hepatoma cells (*c* and *d*). (*c*) Spot radius, 0.6 μm (40× objective). Average mobile fraction is 0.42 ± 0.10. $D = 8 \times 10^{-10}$ cm$^2 \cdot$s^{-1}. (*d*) Spot radius, 1.1 μm (22× objective). Average mobile fraction is 0.46 ± 0.14. $D = 21 \times 10^{-10}$ cm$^2 \cdot$s^{-1}.

The data presented here extend our operational definition of membrane domains to the surface of K78-2, mouse hepatoma, cells. R and D of NBD-PC in these cells show a dependence on spot size as they did in human fibroblast membranes over a range of laser spot radii from 0.3 to 2.0 μm. In this range R varied from ~0.8 to ~0.25 and D varied from $\sim 1 \times 10^{-10}$ to $\sim 25 \times 10^{-10}$ cm$^2 \cdot$ s^{-1}. As is the case in fibroblast membranes another fluorescent lipid analog, the indocarbocyanine dye dil C16, does not show this behavior. The relatively small difference in D of dil C16 measured at two different spot sizes could be largely accounted for by small errors (10–15%) in measurement of the laser beam radius.

Two different class I MHC molecules are expressed at the surface of K78-2 hepatoma cells. One, an endogenous class I molecule, H-2D^b, is anchored to the membrane bilayer through a transmembrane peptide of 23 residues; a cytoplasmic tail of 27 residues follows this transmembrane domain. The other class I molecule, Qa-2, the product of a transfected Q7 gene, is >80% homologous to H-2D^b, but is anchored to the membrane through a phosphatidylinositol glycan, GPI, which only extends into the outer leaflet of the bilayer. The expression of the two homologous proteins in one cell membrane resolves the effects of a GPI anchorage on lateral diffusion behavior in a way that has not been possible in published measurements of the lateral diffusion of GPI-linked proteins (Cowan et al., 1987; Ishihara et al., 1987; Phelps et al., 1988). Though membrane anchorage by GPI is not reflected in differences between the diffusion coefficients of the H-2D^b and Qa-2 molecules, it is evident in the ways in which the molecules are constrained in their lateral mobility. The apparent mobile fraction, R, of the peptide-anchored H-2D^b molecule depends upon the size of the laser spot

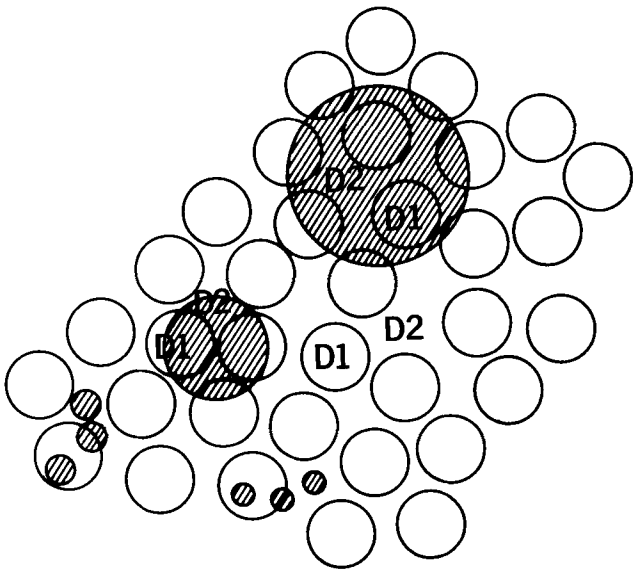

Figure 8. A schematic model of membrane domains. Illuminated areas, which may be larger or smaller than the area of a domain, are shaded. Domains are indicated as circles. *D* of a given molecule is *Dl* (<*D2*) in the bounded, protein-rich domains and *D2* in the relatively lipid region between the domains.

used in an FPR measurement, while the mobile fraction of the GPI-anchored protein is independent of spot size. These relationships between spot size and *R* are also true for hybrid class I molecules. A hybrid, K123/12, with the exodomain of Qa-2 and transmembrane and cytoplasmic regions of a conventional class I antigen, H-2D^b appears to be constrained by membrane domains, while a hybrid, K123/13, with a mixture of Qa-2 and H-2D^b domains terminating in the GPI membrane linkage, behaves like the native Qa-2 molecule. *R* does not change with changes in laser spot size.

The diffusion coefficients of both H-2D^b and Qa-2 increased with increasing spot size. However, for a given small spot size *D* for H-2d^b was low when fluorescence intensity, a measure of protein concentration, was high and vice versa while *D* for Qa-2 was not correlated at all with fluorescence intensity.

These results bear on three points: the nature of the regions probed by the NBD-lipid analogue, the locus of constraints to the lateral diffusion of membrane proteins H-2D^b and Qa-2, and the structural basis of the membrane domains defined by our FPR experiments.

In our hands the diffusibility of NBD-PC added to cells by injection of a few microliters of stock solution in ethanol has consistently resembled that of proteins, rather than that of native lipids. In particular *D* measured with our usual small laser spot, radius 0.6–0.8 μm, is in the range of 1–3 $\times$ 10^{-10} cm^2·sec^{-1}, similar to that for many membrane proteins. It is not likely that this behavior is due to the partition of the lipid analogue into gel domains since this class of lipid analogues partitions into fluid phases due to its high water solubility. It may be that this lipid analogue associates with membrane proteins to a greater extent than do lipid analogues such as the indocarbocyanines whose hydrophobic regions are unmodified and which can selectively partition into gel or fluid phases. The capping of NBD-PC reported earlier is consistent with this idea [Schroit and Pagano, 1981]. If this is so then the spatial differentiation of membranes reported by measurements of the lateral diffusion of NBD-PC involves both proteins and lipids and may be dominated by lipid/protein, rather than lipid/lipid, interactions.

The diffusion coefficients, *D* measured for H-2D^b and Qa-2 molecules are comparable for all laser spot sizes used. They are low, in the range 1–5 $\times$ 10^{-10} cm^2 · s^{-1}, for spots of small area, and are 5–20 times larger, in the range 1–30 $\times$ 10^{-10} cm^2 · s^{-1}, when large spots are used. The higher values in this range approach *D* for viscosity-limited diffusion of proteins in lipid bilayers, 50–100 $\times$ 10^{-10} cm^2 · s^{-1}. We have previously shown that in some instances *D* for membrane glycoproteins is largely constrained by interactions between proteins in the plane of the membrane, and not by interactions with the cytoskeleton (Wier and Edidin, 1988). The results here, in which molecules with and without cytoplasmic domains have the same values of *D* are also consistent with this interpretation.

The changes in apparent *D* with increasing spot size cover an even greater range (20–25 times) than those that we observed previously for membrane proteins (Yechiel and Edidin, 1987). This range may reflect the biology and organization of K78-2 surfaces, but it could to some extent be due to any or all of a number of optical artifacts: improper measurement of beam radii produced by different objectives, focusing errors (especially with small spots), slight misalignment of the spot with the aperature used to limit light collection by the photomultiplier, and failure of the electronics to resolves rapid recoveries of fluorescence in very small spots. It is unlikely that the first of these contributes significantly to the observed range of *D*. Our measurements of spot size analyze an expanded image of the beam following a published procedure (Schneider and Webb, 1981) and are sufficiently accurate so that *D*, calculated from $t_{1/2}$, of fluorescent IgG in 98% glycerol solution, is quite similar for all spot sizes examined and is within 20% of the value calculated from published values for IgG diffusion in water and the measured viscosity of the glycerol solution. Critical focusing, though difficult, is easiest for high NA, high magnification, objectives; hence, it is unlikely to produce gross errors, of the magnitude (about threefold) required to give the observed range of *D*. Judging from some published work, a defocus of $\sim$2 μm would be required to increase the spot size threefold (Hiraoka et al., 1990).

The third and fourth artifacts mentioned may be important. In model systems we can see clearly that misalignment of spot to aperature can cause a lag in the observed recovery. Such a lag could mask rapid recoveries. Alignment of the spots is checked daily and each time the spot size is changed. It is unlikely to be a major contributor to our results. Resolution of very fast recoveries is potentially a great problem for our results. However, we have found that the smallest spots that we can produce, 0.35–0.45 μm, can resolve recoveries when *D* is <2 $\times$ 10^{-9} cm^2 · s^{-1} and slightly larger spots, 0.6–0.7 μm, can resolve recoveries when *D* is $\sim$5 $\times$ 10^{-9} cm^2 · s^{-1}. Hence, it is likely that the *D* measured with small spots reflects membrane biology rather than being due to optical artifacts. Another group have also found that *D* of a membrane protein measured with small spots (0.8 μm radius) is five- to sixfold smaller than *D* measured with spots of 2–4 μm radius [Dubinsky et al., 1989]. This group suggested that recoveries on short time scales are dominated by

the times of interaction of the diffusing molecules with constraints; either immobile membrane proteins or proteins of the cytoplasm.

The mobile fraction of Qa-2 was ~0.5 for all measuring spot sizes and was not changed by interferon treatment of the cells; the mobile fraction of H-2D^b was never higher than ~0.6. Though the low apparent mobile fraction is due in part to a small fraction of nonspecifically bound fluorescence and to cellular autofluorescence (both of which bleach but do not recover), most of it is due to specifically labeled class I molecules that are immobile on the time scale of an FPR experiment. Similar immobile fractions, from 20 to 70% of a population of molecules are found for other inositol lipid-linked proteins as well as for peptide-anchored membrane proteins (reviewed in Edidin, 1990*b*).

Our most important experimental criteria for locating a molecule in membrane domains are the relationship between R and spot size, and the relationship between D and concentration of labeled molecules. The results obtained on H-2D^b molecules fit these criteria. R decreases with increasing spot size, and for small spots D is lower in spots of higher protein concentration than in spots of lower protein concentration (measured as fluorescence intensity). These relationships are consistent with our previous model in which proteins are enriched in membrane domains of micrometer scale which are surrounded by a continuum of relatively protein-poor membrane (Fig. 8). The results on Qa-2 molecules do not fit our criteria, but they lead to further definition of the model of Fig. 8. Since the main difference between H-2D^b and Qa-2 is in their mode of anchorage to the bilayer and the extent of their interaction with the cell cytoplasm we propose that the domains detected in our experiments arise from interactions of membrane proteins with cell cytoskeleton. Further experimental evidence for the importance of the cytoplasmic tail in concentrating proteins in domains comes from our results on mutant proteins. Molecules with the external portion of Qa-2 but linked to the bilayer by a transmembrane peptide with a cytoplasmic tail appear by our criteria to be concentrated in domains. Hybrid class I molecules with a significant portion derived from a peptide-linked, classical, class I antigen, but linked to the bilayer by GPI do not appear to be concentrated in membrane domains. It appears that proteins without a cytoplasmic tail cross the boundaries of membrane domains more readily than molecules carrying transmembrane and cytoplasmic segments. However, diffusion of GPI-linked proteins within membrane domains is impeded by a high concentration of membrane proteins.

On this interpretation D for Qa-2 ought to be a mixture of $D1$, for diffusion within a protein-rich domain, and $D2$, for diffusion in the continuum, relatively poor in proteins, between the domains. If the area of the domains is greater than that of the continuum between them, then most FPR measurements with small laser spots will give recovery curves dominated by $D1$. Small spots falling on regions outside the domains $D = D2$ will result in truncated recovery curves if $D2$ is $> 2 \times 10^{-9}$ cm$^2 \cdot$ s^{-1}. Measurements using large spots will give recoveries dominated by $D2$, diffusion of Qa-2 molecules in the continuum, but molecules diffusing at $D1$, within domains will also contribute. The mixture of recoveries will underestimate $D2$ and the total recovery. The extent of the error depends upon the magnitudes of $D1$ and $D2$ and on their fractional contributions, $p1$ and $p2$, to the recovery curve, but it appears that even a large fraction of $D1$ will have a small effect. For example, let us take $D2 = 5 \times 10^{-9}$ cm$^2 \cdot$ s^{-1}, p2 = 0.33; $D1 = 2.5 \times 10^{-10}$ cm$^2 \cdot$ s^{-1}; $p1 = 0.67$ and a spot radius, $w^2 = 1.3$ μm. With these values of w^2 and $D2$, $t_{1/2}$ is ~1 s and one-third of the total recovery will occur in ~5 s. The rest of the recovery will be due to molecules diffusing at $D1$. $t_{1/2}$ for this recovery is ~20 s. Very roughly the total recovery (with contributions by both populations of molecules) will be 45% of maximum at 5 s, 50% at 10 s, 67% at 20 s, and 83% at 40 s. The fit of such a curve by our program would be close to the fit for a single component recovery.

Our results extend the experimental definition of membrane domains previously made for proteins of human fibroblasts to class I proteins of hepatoma cells. They further suggest that the basis for these domains lies in the inner leaflet of the bilayer or in the cell cytoplasm. The scale of the domains appears to be in micrometers. Such a scale could be imposed by the spacing of stress fibers in fibroblasts [for example see Bershadsky and Vasiliev, 1988] or by a spectrin (fodrin) cytoskeleton. The mesh of spectrin tetramers observed in the erythrocytes has dimensions of ~0.2 μm per side (Shen et al. 1986; Liu et al., 1987). Imperfect meshes or patches of mesh separated by spectrin-free regions could form the basis for the organization of cell surfaces into domains. If such patches are coupled to the lipid bilayer and exert lateral pressure on the bilayer lipids they could also serve to induce lipid/lipid immiscibilities that are the basis for other sorts of membrane domains, for example those detected by the indocarbocyanine dyes such as diI C16. Both protein diffusibility and lipid domain formation would be modulated by fluctuations in the spectrin assembly (Saxton, 1990).

We thank Mrs. K. Blackburn and Mrs. Taiyin Wei for technical assistance.

This work was supported by National Institutes of Health grants AI14584 (M. Edidin) and AI17565 (I. Stroynowski).

Received for publication 1 August 1990 and in revised form 1 December 1990.

References

Bershadsky, A. D., and J. M. Vasiliev. 1988. Cytoskeleton. Plenum Publishing Corp. New York. 298 pp.

Bierer, B., S. H. Herrmann, C. S. Brown, S. J. Burakoff, and D. E. Golan. 1987. Lateral mobility of class I histocompatibility antigens in B lymphoblastoid cell membranes: modulation by cross-linking and effect of cell density. *J. Cell Biol.* 105:1147–1152.

Bjorkman, P. J., M. A. Saper, B. Samroui, W. S. Bennett, J. L. Strominger, and D. C. Wiley. 1987. Structure of the human class I histocompatibility antigen, HLA-A2. *Nature (Lond.).* 329:506–511.

Cowan, A. E., D. G. Myles, and D. E. Koppel. 1987. Lateral diffusion of the PH-20 protein on guinea pig sperm: evidence that barriers to diffusion maintain plasma membrane domains in mammalian sperm. *J. Cell Biol.* 104: 917–923.

Darlington, G. J., H. P. Bernhard, R. A. Miller, and F. H. Ruddle. 1980. Expression of liver phenotypes in cultured mouse hepatoma cells. *J. Natl. Cancer Inst.* 64:809–817.

Dubinsky, J., D. J. Loftus, G. D. Fischbach, and E. L. Elson. 1989. Formation of acetylcholine receptor clusters in chick myotubes: migration or new insertion? *J. Cell Biol.* 109:1733–1743.

Edidin, M. 1990*a*. Molecular associations and membrane domains. *Curr. Top. Membr. Trans.* 36:81–93.

Edidin, M. 1990*b*. Translational diffusion of membrane proteins. *In* The Structure of Biological Membranes. P. Yeagle, editor. Telford Press, Caldwell, NJ. In press.

Hiraoka, Y., J. W. Sedat, and D. A. Agard. 1990. Determination of the three-dimensional imaging properties of a light microscope system. Partial confocal behavior in epifluorescence microscopy. *Biophys. J.* 57:325–333.

Ishihara, A., Y. Hou, and K. Jacobson. 1987. The Thy-1 antigen exhibits rapid lateral diffusion in the plasma membrane of rodent lymphoid cells and fibroblasts. *Proc. Natl. Acad. Sci. USA.* 84:1290–1293.

Karnovsky, M. J., A. M. Kleinfeld, R. L. Hoover, and R. D. Klausner. 1982. The concept of lipid domains in membranes. *J. Cell Biol.* 94:1–6.

Klausner, R. D., and D. E. Wolf. 1980. Selectivity of fluorescent lipid analogues for lipid domains. *Biochemistry.* 19:6199–6203.

Klausner, R. D., A. M. Kleinfeld, R. L. Hoover, and M. J. Karnovsky. 1980. Lipid domains in membranes: evidence derived from structural perturbations induced by free fatty acids and lifetime heterogeneity analysis. *J. Biol. Chem.* 255:1286–1295.

Liu, S. C., L. H. Derick, and J. Palek. 1987. Visualization of the hexagonal latticed in the erythrocyte membrane skeleton. *J. Cell Biol.* 104:527–536.

Ozato, K., and Sachs, D. 1980. Monoclonal antibodies to mouse MHC antigens III. Hybridoma antibodies reacting to antigens of the H-2^b haplotype reveal genetic control of isotype expression. *J. Immunol.* 126:317–321.

Phelps, B. M., P. Primakoff, D. E. Koppel, G. M. Low, and D. G. Myles. 1988. Restricted lateral diffusion of PH-20, a PI-anchored sperm membrane protein. *Science (Wash. DC).* 204:1780–1782.

Rodriguez-Boulan, E., and W. J. Nelson. 1989. Morphogenesis of the polarized epithelial cell phenotype. *Science (Wash. DC).* 245:718–725.

Saxton, M. J. 1990. The membrane skeleton of erythrocytes. A percolation model. *Biophys. J.* 57:1167–1177.

Schneider, M. B., and W. W. Webb. 1981. Measurement of submicron laser beam radii. *Appl. Opt.* 20:1382–1388.

Schroit, A. J., and R. E. Pagano. 1981. Capping of a phospholipid analog in the plasma membrane of lymphocytes. *Cell.* 23:105–112.

Shen, B. W., R. Josephs, and T. L. Steck. 1986. Ultrastructure of the intact skeleton of the human erythrocyte membrane. *J. Cell. Biol.* 102:997–1006.

Stroynowski, I. 1990. Molecules related to class-I major histocompatibility complex antigens. *Annu. Rev. Immunol.* 8:501–530.

Stroynowski, I., M. Soloski, M. G. Low, and L. E. Hood. 1987. A single gene encodes soluble and membrane bound forms of the major histocompatibility Qa-2 antigen: anchoring of the product by a phospholipid tail. *Cell.* 50:759–768.

Thompson, T. E., and T. W. Tillack. 1985. Organization of glycosphingolipids in bilayers and plasma membranes of mammalian cells. *Annu. Rev. Biophys. Biophys. Chem.* 14:361–386.

Ulker, N., L. E. Hood, and I. Stroynowski. 1990. Molecular signals for phosphatidylinositol modification of the Qa-2 antigen. *J. Immunol.* 145:2214–2219.

Wier, M. L., and M. Edidin. 1988. Constraint of the translational diffusion of a membrane glycoprotein by its external domains. *Science (Wash. DC).* 242:412–414.

Wolf, D. E., and M. Edidin. 1981. Diffusion and mobility of molecules in surface membranes. *In* Techniques in Cellular Physiology. P. F. Baker, editor. Elsevier Biomedical, New York. P105:1–14.

Wolf, D. E., W. Kinsey, W. Lennarz, and M. Edidin. 1981*a*. Changes in the organization of sea urchin egg plasma membrane upon fertilization: indications from the lateral diffusion rates of lipid-soluble dyes. *Dev. Biol.* 81:133–138.

Wolf, D. E., M. Edidin, and A. H. Handyside. 1981*b*. Changes in the organization of the mouse egg plasma membrane upon fertilization and first cleavage: indications from lateral diffusion rates of fluorescent lipid analogs. *Dev. Biol.* 85:195–198.

Wolf, D. E., A. C. Lipsomb, and V. M. Maynard. 1988. Causes of nondiffusing lipid in the plasma membrane of mammalian spermatozoa. *Biochemistry.* 27:861–865.

Yechiel, E., and M. Edidin. 1987. Micrometer-scale domains in fibroblast plasma membranes. *J. Cell Biol.* 105:755–760.